Hittite Journal of Science and Engineering, 2017, 4 (1) 07-16
ISSN NUMBER: 2149-2123
DOI: 10.17350/HJSE19030000042

Thermal Grooving by Surface Diffusion: a Review of Classical Thermo-Kinetics Approach

Oncu Akyildiz[1], and Tarik Omer Ogurtani[2]
[1]Department of Metallurgical and Materials Engineering, Hitit University, 19030, Corum, TURKEY.
[2]Department of Metallurgical and Materials Engineering, Middle East Technical University, 06531, Ankara, TURKEY.

ABSTRACT

In polycrystalline materials wherever a grain boundary intersects a free surface and whenever the topographic variation associated with the atomic motion is favored by total free energy dissipation, the material surface grooves. In this review, we focused on the grain boundary grooving by surface diffusion which is an active mechanism at moderate temperatures and for grooves small in size. Starting with a description of the classical thermo-kinetics treatment of the process, we briefly reviewed Mullins' very first modeling effort with a small slope assumption at the groove root and further considerations regarding finite slopes, different grain geometries, and anisotropic surface free energies. We concluded by giving examples of experimental observations in accord with theoretical calculations.

Article History:
Received: 2016/10/17
Accepted: 2016/12/02
Online: 2017/06/30

***Correspondence to**: O Akyildiz, Department of Metallurgical and Materials Engineering, Hitit University, 19030, Corum, TURKEY*
Tel: +90 364 227 4533/1282;
Fax: +90 364 227 4535
E-Mail: oncuakyildiz@hitit.edu.tr

Keywords: *Thermal grooving; Grain boundary groove; Surface diffusion*

INTRODUCTION

Polycrystalline materials are composed of tiny perfect crystalline regions (grains) in between internal interfaces called grain boundaries. Grain boundaries and the external interfaces (i.e. free surfaces which separate the material from the environment) determine the morphology of the material at a major extent.

A material may change its morphology through interface motion if a driving force exists. An important special case, which is the focus of this review, is the grain boundary grooving. Wherever a grain boundary intersects a free surface and whenever the topographic variation associated with the atomic motion is favored by total free energy dissipation, the surface grooves. Grooving can occur via several mass transport mechanisms, such as surface diffusion, bulk diffusion, and evaporation and condensation. Surface diffusion dominates for temperatures far below the melting temperature, and for grooves less than 10 micron in size [1]. If the surface evolution is driven solely by the total excess free energies associated with the interfaces the resulting force for motion is conventionally called a capillary force, and the new formation is termed as a *thermal groove*. In addition to a capillary force, a force for interface motion is produced whenever motion of the interface allows an applied force to perform work: such a force is an applied force [2].

A major portion of the literature on morphological evolution solid surfaces and interfaces mainly rely on classical thermodynamics. The idea is to minimize the free energy of the system by suitable mechanism of mass transport. Considering systems at equilibrium a driving force is determined from the total free energy variation, and a linear kinetic law is used to relate the driving force to the flux. Using this flux, surface shape is updated according to mass conservation.

Mullins [3] successfully cast this approach to the problem of thermal grooving in 1957 by imposing suitable boundary conditions and provide an analytic solution which provides groove profile as a function of time and position under some assumptions. After that time several improvements has been done by several researchers who follow the classical approach. In this review

article we will briefly discuss these concepts and conclude by giving examples of experimental observations compared with theoretical calculations.

It should also be mentioned that this review reflects authors' personal perspective on this specific (yet still broad enough) part of the broader topic of thermodynamics and kinetics of solid surfaces and interfaces.

Classical thermo – kinetics theory

Kinetics of morphological changes by surface diffusion

It is useful to outline the surface diffusion driven motion of an arbitrary surface before proceeding further into the detailed literature review. The atomic flux (vector field; the bar signs over symbols are to denote vector quantities) on such a solid surface given in figure 1 may be defined at a per length basis by:

$$\vec{J}_\sigma = \frac{\#\text{ of atoms}}{(\text{length})(\text{time})} \tag{1}$$

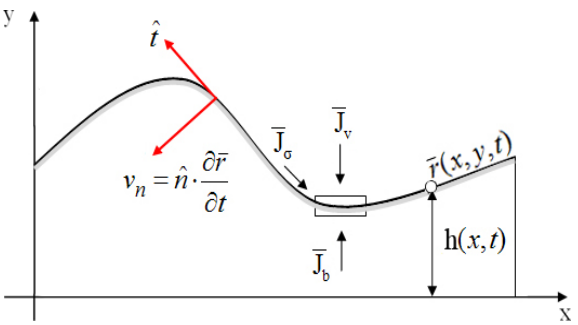

Figure 1. An arbitrary surface in the x-y plane. $\hat{t}$ is the unit tangent and $\hat{n}$ is the unit normal vector, the subscripts σ, b, v on the fluxes denote the surface, bulk, and void phases respectively. When evaporation condensation mechanism is active, J_b and J_v entering (leaving) the surface element should also be considered. At a given time any point on the surface may be represented by position vector $\vec{r}(x,y)$.

When a surface element gains atoms, it moves with a velocity v_n (scalar field) in the direction normal to the surface. Defining Ω as the volume per atom in the solid the ratio v_n/Ω gives the atoms gained per unit area per unit time. This quantity is related to the flux divergence through conservation of mass:

$$\frac{v_n}{\Omega} + \nabla \cdot \vec{J}_\sigma = 0 \quad \text{(the continuity equation)} \tag{2a}$$

$$v_n = -\Omega \nabla \cdot \vec{J}_\sigma \tag{2b}$$

Once the diffusion flux is obtained surface can be evolved using the velocity calculated by this equation. The atomic flux on the surface can be related to the driving force for diffusion through atomic mobility M by using a linear kinetic law [4, 5]:

$$\vec{J}_\sigma = M\vec{F} \tag{3}$$

This connection is a typical consequence of linear irreversible thermodynamics as underlined by Sun and Suo [4, 5] and adopted by Herring [6] and Mullins [3].

The literature of diffusion controlled surface morphological changes is fulfilled by the following concept: the driving force in Eq. (3) may be interpreted as a gradient energy which is everywhere continuous even at the singularities; otherwise the flux might go to infinity. The assumed surface diffusion potential is a scalar field that reflects a change in energy that results from the motion of species; therefore, it includes energy-storage mechanisms and any constraints on motion [2]. Therefore all efforts start with a definition of the term surface chemical potential, μ_σ whose gradients drive the overall processes.

Following Herring, the driving force in Eq. (3) is a vector on the interface that is derived from gradient of a scalar field which has units of energy per atom. If atoms diffuse from an interfacial element with high potential to another with low potential, then the driving force is the negative gradient of the surface diffusion potential μ_σ:

$$\vec{F} = -\nabla\mu_\sigma \tag{4}$$

Substituting Eqs. (4⟶3⟶2) and assuming a position independent atomic mobility one can relate the normal velocity of the free surface to the Laplacian of the surface diffusion potential:

$$v_n = \Omega M \nabla^2 \mu_\sigma \tag{5}$$

Another common representation of Eq. (5) may be obtained by the following form of the Nernst – Einstein equation which ties the mobility and surface self-diffusivity, D_σ:

$$M = \frac{h_\sigma}{\Omega}\frac{D_\sigma}{kT} \tag{6}$$

Here h_σ is the thickness of the surface layer, k is the Boltzmann constant and T is the absolute temperature. Substitution Eq. (6⟶5) yields:

$$v_n = \frac{D_\sigma h_\sigma}{kT}\nabla^2\mu_\sigma \tag{7}$$

Energetics of morphological changes by surface diffusion

If there is no exchange of energy between the solid and its surroundings then the change in free energy for a given change in shape represents the driving force for that shape change (Eq. 4). So, the next step is to obtain a proper definition for the total free energy that could be used in connection with Eq. (7). The very first study in this field came from Herring in 1951 which strictly rely on the equilibrium thermodynamics and the Gibbs description of interfaces and surfaces [7, 8]. He extends the classical Gibbs-Thomson equation for an orientation dependent surface tension γ_s, as in a crystal.

Herring's equation of curvature dependent chemical potential

The Gibbs-Thomson equation reflects typical consequence of the dependence of equilibrium vapor pressure of a liquid drop on its radius of curvature; i.e. it relates the curvature of a surface to the chemical potential of the surface atoms when surface tension γ_s, is independent of orientation. Herrings theory, in a similar way, assumes that the free energy of the system is the surface energy summed over all surfaces and grain boundaries, and the amount of free energy decrease is associated with per unit volume of matter moving per unit distance on the surface and as a result describes a driving force at every point on the solid surface.

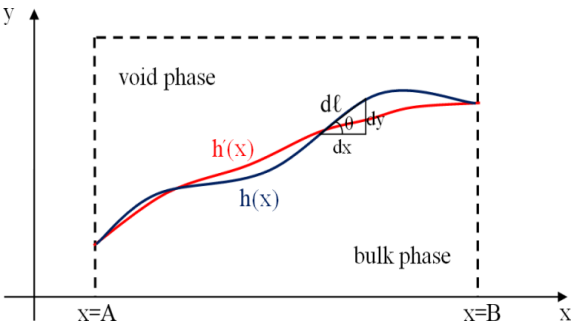

Figure 2: The curve h(x) between x=A and B represents a portion of the cross section of a surface between bulk and void phases. h´(x) is the surface perturbed by an infinitesimal amount ´h(x).

Mullins [9] gives a derivation of Herring's equation using calculus of variations in two dimensions by considering a monocomponent system, under no applied pressure. In such a system surface tension γ_s, is equal to the specific surface free energy, f_σ. Then the value of the surface free energy, F associated with the curve in figure 2 from A to B, per unit depth, is given by the following line integral:

$$F_\delta = \int_A^B \gamma_s d\ell = \int_A^B \gamma_s(h_x)\sqrt{1+h_x^2}\,dx = \int_A^B G(h_x)\,dx \qquad (8)$$

Here h_x represents differentiation with respect to x; simply it is the slope of the curve at any point and used as an argument for γ, since it determines the orientation of the surface element. Then if an infinitesimal rearrangement of material forms the new surface: h´(x)=h(x)+δh(x). The corresponding variation in F_σ is obtained by calculus of variations as:

$$\delta F_\delta = \int_A^B \frac{dG}{dh_x}\delta h_x dx = \int_A^B \frac{dG}{dh_x}\frac{d(\delta h)}{dx}dx = -\int_A^B \frac{d}{dx}\left(\frac{dG}{dh_x}\right)\delta h dx \qquad (9)$$

Here for simplicity δh(A)= δh(B)=0 and $\int_A^B \delta h(x)\,dx = 0$. Assuming the chemical potential $\mu'_\delta = \mu_\delta + \mu_0$ to be uniquely determined at all elements of the surface apart from the constant μ_σ, δF must also be given by the following expression:

$$\delta F_\delta = \frac{1}{\Omega}\int_A^B (\mu_\delta + \mu_0)\delta h dx = \frac{1}{\Omega}\int_A^B \mu_\delta \delta h dx \qquad (10)$$

Here, μ_σ is defined as the chemical potential at standard state which can arbitrarily be assigned to the value zero in the reservoir, Ω is the atomic volume and δhdx/Ω gives the number of atoms added to the interval dx. Subtracting Eq. (9→10):

$$0 = \int_A^B \left\{\frac{d}{dx}\left(\frac{dG}{dh_x}\right) + \frac{\mu_\delta}{\Omega}\right\}\delta h dx \qquad (11)$$

Since δh is arbitrary:

$$\mu_\delta = -\Omega\frac{d}{dx}\left(\frac{dG}{dh_x}\right) = -\Omega\frac{d}{dx}\left(\frac{d}{dh_x}\left(\gamma_s(h_x)\sqrt{1+h_x^2}\right)\right) \qquad (12)$$

Using following equalities in performing differentiations:

$$\theta = \arctan(h_x) \qquad \frac{d\gamma_s}{dh_x} = \frac{1}{1+h_x^2}\frac{d\gamma_s}{d\theta} \qquad \frac{d}{dx} = h_{xx}\frac{d}{dh_x}$$

Eq. (12) yields:

$$\mu_\delta = -\Omega\left(\gamma_s + \frac{d^2\gamma_s}{d\theta^2}\right)\frac{h_{xx}}{\left(1+h_x^2\right)^{3/2}} = \Omega\left(\gamma_s + \frac{d^2\gamma_s}{d\theta^2}\right)\kappa \qquad (13)$$

Here, $\kappa = -h_{xx}\left(1+h_x^2\right)^{-3/2}$ is the curvature at a point on the surface and taken to be positive when the surface is concave towards the bulk. For isotropic γ, as in liquids, Eq. (13) directly reduces to Gibbs-Thomson equation. Substituting Eq. (13) into (7), one may specify a governing differential equation for capillarity induced evolution of surfaces and interfaces.

Mullins' theory of thermal grooving

Thermal grooving at grain boundaries is a process of capillary – driven evolution of surface topography in the region where a grain boundary emerges to intersect a free surface of a polycrystalline material. Mullins [3] derived a general PDE for the rate of change of the profile of a surface for profile changes occurring by surface diffusion mechanism under the following assumptions:

(1) The system is closed and contains a metal poly-crystal in quasi-equilibrium with its vapor.
(2) Interface properties are independent of crystallographic orientation.
(3) All matter transport occurs by surface self-diffusion.
(4) Macroscopic concepts such as surface free energy and curvature are valid.
(5) There is negligible flow of matter out of the grain boundary; instead, the role of the boundary is to maintain the correct equilibrium angle.
(6) Absolute value of the profile slope is everywhere small compared to unity; the small slope assumption (SSA).

Under these assumptions he follows the very same procedure described above (Eq. 13→7) and obtains following equation:

$$v_n = \frac{D_\sigma \gamma_s \Omega^2 \nu}{kT} \nabla^2 \kappa \tag{21}$$

Here, Mullins adopted $\nu = h_\sigma / \Omega$ as the number of per unit area, instead of using h_σ itself. Owing to isotropy he collects all physical constants into one ($B=D_\sigma \gamma_s \Omega^2 \nu/kT$) and rewrites Eq. (21) explicitly in terms of h(x,t):

$$\frac{\partial h}{\partial t} = -B \frac{\partial}{\partial x}\left(\left(1+h_x^2\right)^{-1/2} \frac{\partial}{\partial x}\left(h_{xx}\left(1+h_x^2\right)^{-3/2} \right) \right) \tag{22}$$

This nonlinear PDE is in fourth order in space and hard to solve analytically. Mullins linearized this equation referring to the assumption (6) given above: slope of the surface is everywhere small compared to unity.

$$\frac{\partial h}{\partial t} = -B h_{xxxx} \tag{23}$$

He considers a symmetrically disposed stationary grain boundary at x=0 that is perpendicular to the free surface as in Figure 3. Then he formulates the following initial and boundary conditions:

$$h(x,0) = 0 \tag{24a}$$

$$h_x(0,t) = \tan\theta = m \ll 1 \tag{24b}$$

$$J_{gb}(0,t) = h_{xxx}(0,t) = 0 \tag{24c}$$

$$h(\pm\infty,t) = h_x(\pm\infty,t) = 0 \tag{25d}$$

Eq. (1.4.4a) is an initial condition for the problem and assumes an initially flat surface. Eqs. (1.4.4b, c) are the boundary conditions for the triple junction; the first one fixes the dihedral angle ($\phi=\pi-2\theta$) at the groove root through mechanical equilibrium ($sin\theta=\gamma_{gb}/2\gamma_s=\lambda$; where λ may be called as the wetting parameter) and the second sets the flux of atoms out of the boundary to zero. And 1.4.4d assures that flat surface remote from the triple junction at all time.

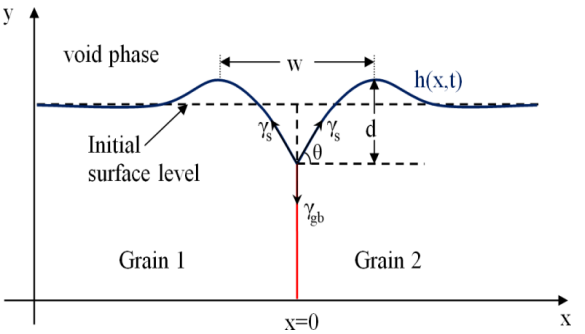

Figure 3. Sketch of the curve h(x,t); the surface profile function. d is the groove depth measured from the maxima and w is the separation between the two maxima, namely the groove width. γ_{gb} and γ_s are the grain boundary and surface tensions respectively. $\phi = \pi - 2\theta$ is the equilibrium dihedral angle, force balance requires $2\gamma_s \sin\theta = \gamma_{gb}$ at the groove root.

Mullins [57] obtains an analytic solution of Eq. (23) subjected initial and boundary conditions defined in Eqs. (24) as:

$$y(u,t) = m(Bt)^{1/4} Z(u) \quad \text{with}$$

$$u = \frac{x}{(Bt)^{1/4}} \quad \text{and} \quad Z(u) = \sum_{n=0}^{\infty} a_n u^n \tag{25a}$$

$$a_0 = \frac{-1}{\sqrt{2}\Gamma(5/4)};\ a_1 = 1;\ a_2 = \frac{-1}{2\sqrt{2}\Gamma(3/4)};\ a_3 = 0;$$
$$a_{n+4} = a_n \frac{n-1}{4(n+1)(n+2)(n+3)(n+4)} \tag{25b}$$

Here, Γ is the gamma function. It is inferred from Eq. (25) that the groove shape is dependent upon the material constant $m=tan\theta$; but is independent of time and the physical parameters comprising *B*. Mullins [3] stated that the groove instantly attains a constant shape whose linear dimensions grow in proportional to $t^{1/4}$, and deduce two technically important equations:

$$d=0.973m(Bt)^{1/4} \tag{26a}$$

$w=4.6(Bt)^{1/4}$ (26b)

The first kinetic equation stands for the steady shape grooves' depth, d and second for its width, w (see Fig. 3). These two equations give possibility to determine surface diffusion constants experimentally

After Mullins' publication [3] in 1957 considerable amount of work had been dedicated by several investigators to obtain a solution that accounts finite slopes at the groove root; some of them will be cited here. Robertson [10] transforms the nonlinear PDE to an ordinary differential equation of *Z(u)* by inserting Eq. (25a) to Eq. (22) and numerically integrates it to obtain solutions for finite slopes ranging from 0 to 4. He found groove depths lower than estimated by Eq. (26a) for finite slopes. Zhang & Schneibel [11] use method of lines approach to solve Eq. (22); Khenner et al. [12] categorize the problem as a two dimensional initial boundary value problem of type Hamilton-Jacobi and proposed a numerical solution by using a level set method. Both articles address and discuss several numerical methods to solve the nonlinear PDE. The conclusion shared is that the groove profile stays self similar; the width and height of the groove grow with time t as $t^{1/4}$ as predicted by Mullins' small slope solution.

Several cases regarding to geometry had also been studied in the literature. Mullins theory assumes an isolated groove and it can be inferred from his solution that every film subjected to a long enough annealing time will rupture. Hackney & Ojard [13] consider an array of equally spaced parallel grain boundaries with the same symmetric contact angle (Fig. 4a) under SSA. They employ following boundary conditions:

$$h_x(R,t) = h_x(-R,t) = \tan\theta = m \ll 1 \quad (27a)$$

$$J_{gb}(R,t) = h_{xxx}(R,t) = 0 \quad (27b)$$

$$h_x(0,t) = 0 \quad (27c)$$

The third one is the symmetry condition at the center of the grain, whilst the others are self explanatory for a groove root placed to a distance R. They gave an analytic solution for Eq. (23) that accounts finite grain size 2R. Later Zhang and Schneibel [11] and Khenner [14] studied the very same system by solving Eq. (22) numerically. Both authors observe termination of grooving at long times after formation of identical circular arcs that connect adjacent grain boundaries; a result anticipated long time ago by Srolovitz and Safran [15] merely from energetic calculations. They show that a groove may go to a finite depth even after an infinite time to anneal and estimate the conditions under which film rupture happens (groove divides the bicrystal into two pieces; and therefore give rise to island formation on a substrate) as a function of film aspect ratio ($2R/w_0$; see Fig. 22) and dihedral angle.

Huang et al. [16] consider a different set of boundary conditions for the end points that are free to move in lateral direction to account finite plate like grains that have semicircular ends (constituting a closed loop, Fig. 4b). Through large number of finite element analyses they have deduced an empirical formula that relates minimum dihedral angle (below which no splitting occurs) to the film aspect ratio.

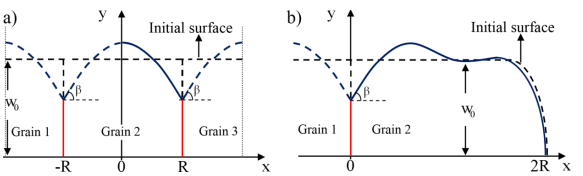

Figure 4. Schematic representation of a) continuous array of grains, b) plate like grains that have semicircular ends. Symmetry prevails due to assumed isotropic surface properties and solution for the solid lines is enough for interpretation.

Ogurtani and Akyildiz [17] utilize three different; reflecting, interactive (Fig. 4a) and free moving (Fig. 4b) boundary conditions and perform thermal grooving simulations on tilted and normal grain boundaries. Yet, their way of treating the triple junction singularity was completely different from those cited here and based on a mathematical model which flows only from fundamental postulates of irreversible thermodynamics. They showed existence of a transient regime and incorporated this regime into their penetration depth formula by stating that the rate of this transient evolution process obeys the first order reaction kinetics. They stated that this regime is totally ignored by researchers employing Mullins' boundary condition at groove root (constant slope).

Surface energy anisotropy

Maybe the most serious simplification made in the Mullins model is the assumption of the full isotropy of the surface energy. Obviously, this assumption justifies the use of the continuum approach, with the macroscopic curvature as the only driving force for surface diffusion. However, the importance of the surface free energy anisotropy in determining the dihedral angle of the groove and the groove shape was recognized soon after Mullins' work. Grain boundary grooves can develop facets due to anisotropic surface energy. The presence of facets on surfaces of grooves poses intricate modeling issues.

The value of surface energy per unit area of a given crystallographic surface orientation is determined by the fine scale structure of that surface. For a high symmetry

orientation in a crystal the surface is atomically flat. For other orientations close to this surface, the structure usually consists of flat terraces with well-defined local surface energies, separated by atomic scale ledges or steps as illustrated schematically in Figure 5. The steps alter the macroscopic surface energy by an amount corresponding to their energy of formation in the configuration relevant to the structure. Below a characteristic roughening transition temperature T_R, "a nominally flat surface of a crystal that is misoriented by a small angle from a high symmetry direction consists of a train of straight parallel steps" [18]. At finite temperature, such "vicinal" surfaces can be stable and can appear on rounded edges on the equilibrium crystal shape.

With increasing temperature, the rounded regions grow at the expense of facets and at T_R (usually below the melting temperature) the surface becomes smoothly rounded as illustrated schematically in Figure 6. Below T_R, "in the Wulff construction of the surface specific Gibbs free energy, the cusp in the γ-plot or the non-analytic term in the surface tension exists as a result of the finite free energy cost per unit length in the formation of a step". Therefore "the disappearance of facets is connected to disappearance of cusps in the γ-plot, and implies that the step free energy vanishes and free proliferation of steps is expected for $T > T_R$" [19].

Mykura [20] stated that, in the case of a coherent twin

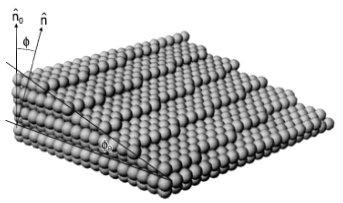

Figure 5. Structure of an fcc $(3\ \bar{2}\ 16)$ surface vicinal to the fcc (001) surface. Figure illustrates zero-temperature steps and kinks that occur on high index (or 'vicinal') surfaces [19].

boundary, the surface anisotropy may even cause the formation of a ridge instead of a groove. Bonzel and Mullins [21] considered the evolution of a pre-perturbed surface topography of the vicinal surface, which is essentially anisotropic. It was found that in the small slope approximation, the flux of the surface atoms is again proportional to the gradient of the surface curvature defined in the proper frame of reference, but should be substituted by a complex expression which depends on the energy of an isolated step, the energy of interaction between steps and the direction of perturbation.

The grain boundary grooving at the singular surfaces were extensively studied by Rabkin et al. [22], Klinger and Rabkin [23], Rabkin and Klinger [24] by explicitly introducing faceted and rough regions, each with different isotropic

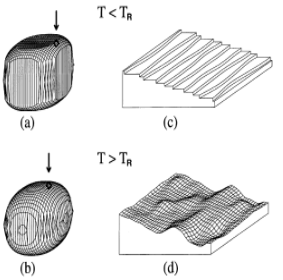

Figure 6. Schematic illustration of equilibrium crystal shapes at finite temperatures, T for a simple cubic model with the nearest neighbor interaction. Equilibrium crystal shapes a) at $T < T_R$: stable (001) facets and b) at $T > T_R$: continuously rounded, have no facet. The regions marked by arrows in a) and b), are vicinal to the low index (001) surface. The difference in mesoscopic structures below and above the roughening temperature is given in c) and d) [19].

surface energies. Zhang et al. [25] derive models describing groove growth while the dihedral angle changes. According to these authors the change in the dihedral angle is caused by the change in the surface energy due to surface contaminations. They express the dihedral angle as a function of time, and after a series of simulations they conclude that changes in the dihedral angle affect the growth exponent for the groove depth much more than the groove width. Growth exponents for depth values as high as 0.4 are possible in this model, whereas Mullins' model predicts an exponent of 0.25 for both the width and depth of the groove. Later Akyildiz et al. [26], analyzed the experimental thermal grooving data reported by these authors, and compared them with their simulation results based on a mesoscopic nonequilibrium thermodynamics treatment. This investigation showed that the observed changes in the dihedral angles are strictly connected to the transient behavior of the simulated global system, and manifest themselves at the early stage of the thermal grooving phenomenon, which is completely overlooked by Mullins' based approach.

Zhang et al. [27] study the effect of anisotropic surface free energy on thermal grain boundary grooving using modeling, simulation and experiments on tungsten. Based on Herring's model they show that, for tungsten, when the anisotropy is mild, the groove profiles are self-similar in the evolution but are often not are in proportion to those developed under isotropic material properties. The grooving kinetics again obeys power law with the exponent 0.25. When the anisotropy is critical surface faceting occurs. And, when it is severe the facets coarsen in the evolution. They exhibit the groove profiles in evolution under different degrees of anisotropy.

Wong and coworkers [28-32] study orientation dependent surface stiffness instead of the surface free energy explicitly in their treatments. They regularize the surface stiffness by replacing the Dirac delta function by sharply peaked functions while former use an analytic form for the

surface free energy which then leads to an analytic surface stiffness and find that faceted grooves still grow with time t with an exponent of 0.25. They stated that, anisotropic groove can be smooth if the groove surface does not cross a facet orientation, moreover the groove has the same shape as the corresponding isotropic groove, but the growth rate is reduced by a factor that depends on the degree of anisotropy. Recently, Ogurtani [33] has reached exactly the same conclusion for the four fold symmetry by applying special analysis on the surface Gibbs free energy function adapted from Ramasubramaniam and Shenoy [34]. The analytic theory developed in conjunction with the extensive computer simulation experiments irrecoverably proved that the smooth grain boundary groove profiles can be represented by the modified Mullins' function [3] with great precision for the symmetrically disposed bicrystal, where the Mullins' rate parameter B is modified by an anisotropy constant Ψ as, $B \Rightarrow B \times (1-\Psi)$ and the isotropic complementary dihedral angle in the slope parameter is replaced by its counterpart in anisotropic case.

Ramasubramaniam and Shenoy [34] made a very serious and successful attempt to obtain a weak solution of the evolution kinetics of faceted grain boundary grooves. They produced proper connections for the TJ displacement velocity that resulted realistic groove root profiles for the symmetrically disposed grain boundary and intersecting surface configurations that are initially flat and infinite in extent. Inspiring from this article, Ogurtani [33] made a unique and transparent treatment of the grain boundary triple junction singularity by the weak solution of the extremum problem imposed by the mathematically more sound Dirichlet boundary conditions to reveal the fine topographic details of the groove root-profiles caused by the non-analyticity of the surface stiffness. In a previous work, Ogurtani [35] elaborates Hermite orthonormal functions manifold by showing that at the asymptotic limit the discrete monolayer representation of the interfaces and surfaces in more realistic Verschaffelt [36] and Guggenheim [37] model may be converged smoothly into the Gibbs abstract model by keeping the intensive variables (specific surface densities) of the interfaces and surfaces invariant and taking the layer thicknesses equal to zero at the limit and extensive variables (contents) infinite. That asymptotic approach, at the expense of the fine features of the grain boundary groove root profiles (rough and faceted regions), was successful not only in eliminating the discontinuity in the particle flux density at the grain boundary triple junction (which results Dirac delta function singularity in the gradient) but also produced most wanted continuity in the derivative of the particle flux density as speculated by Ramasubramaniam and Shenoy [34] to surmount the analytical difficulties. Ogurtani et al. [38] extend this approach to simulate tilted grain boundary grooves in thin metallic films showing four and six fold anisotropy. Later Ogurtani [39] studied the very same problem by employing the modified cycloid-curtate function (MCC) as a basis (generator) for the Dirac delta distribution function on the Wulff construction. This new representation gives more flexibility on the shape of the surface profiles even its temperature dependence by considering not only the intensity but also the topography of the surface Gibbs free energy anisotropy. The utilization of the MCC function also furnished a way for the smooth passage from the soft to sharp faceting morphology by fine tuning the Wulff roughness parameter (anisotropy constant) while keeping topography index invariant.

Experimentally observed thermal grooves

Since its introduction in 1957, Mullins' theory is used extensively in determination of the surface diffusion coefficients (D_s). Once the active mass transport mechanism is confirmed (for evaporation condensation, surface and volume diffusion groove growth obeys $t^{1/2}$, $t^{1/4}$ and $t^{1/3}$ time laws respectively), the ratio of the groove depth (or width) measurements taken at different times yield the B parameter of Eq. (26). As stated before, B is a collection of physical constants: $B=D_s\gamma_s\Omega^2\nu/kT$; providing surface energy γ_s is known, constant temperature experimentation gives the surface diffusivity. Grain boundary grooves are also monitored to measure the dihedral angles and therefore to obtain ratio of surface to grain boundary energies.

Classically, measurements were carried out by electron microscopy or by optical profilometry techniques such as vertical scanning interferometry, phase shifting interferometry, etc. After their invention in the early 1980s, scanning probe microscopies (SPMs) open up new possibilities for studying the surface topography of thermal GB grooves. These instruments combine the possibility to scan relatively large surface areas with atomic resolution in the vertical direction (atomic force microscopy, AFM) and in the case of scanning tunneling microscopy (STM) lateral atomic resolution can be achieved. This makes SPMs ideally suited for the quantitative characterization of surface topography.

Mulins and Shewmon [1] studied grooving kinetics of tilt boundaries in copper by interferometric analysis to show the advantages of the theory in determining D_s. They showed that the dominant process is surface diffusion, and found D_s values in agreement with the ones determined by tracer diffusion studies. A good agreement was also found by Sharma and Spitz [40] for thermal grooves on thin films of silver from a transmission electron microscopy (TEM) study. Tsoga and Nikolopoulos [41] studied grain boundary grooving on polished surfaces of polycrystalline alumina after annealing, in air, under vacuum, and in argon atmospheres in the temperature range 1273 to 1736 K. The

groove angles, measured by optical interferometry, showed no significant change with experimental conditions. It was determined that surface diffusion was the dominant mechanism for the mass transport and the calculated D_s values in agreement with the literature. Tritscher and Broadbridge [42] gave a review of experiments (for diverse materials) where surface diffusion was found to be the dominant mass transfer mechanism.

Several researchers performed AFM studies of thermal grooving. Schöllhammer et al. [43] found excellent agreement between measured and predicted groove shapes for symmetrical tilt grain boundaries in copper. Shin et al. [44] and Lee and Case [45] analyze surfaces of 99.9% alumina samples and report highly asymmetric GB grooves. Rabkin et al. [22] attributed the asymmetry they found for GB grooves in NiAl surfaces to the presence of a vicinal surface on one side of a groove and modified Mullins' [3] linearized equation for thermal GB grooving to take the negligible mass transport on the vicinal surface into account. Qualitative agreement between experimentally observed and calculated groove profiles was found. Rabkin et al. [46] studied the morphologies of GB grooves formed after annealing of molybdenum bicrystals at the temperature close to the melting point with the aid of scanning force microscopy (SFM). Three typical groove morphologies were observed: (i) Mullins-like, albeit asymmetrical grooves with the sharp root; (ii) grooves with the blunted root, and (iii) grooves with the blunted root with the secondary sub-groove with the sharp root in the region of a primary groove. Sachenko et al. [47-49] and Zhang et al. [25, 27] studied GB grooving on the surfaces of polycrystalline tungsten sheets. They found that unfaceted grooves were in qualitative agreement with the predictions of Mullins' theory of grooving by surface diffusion mass transport. They also observed asymmetric grooves between faceted and unfaceted grains showing unusual growth kinetics. Citing these works on tungsten and that of Munoz et al. [50] on alumina, Ogurtani et al. [38] designed special computer simulations and produced surface morphologies at the stationary state which are in excellent agreement with groove profiles measured by AFM and calculated D_s values which are in agreement with the literature.

CONCLUSIONS

Mullins' theory was a milestone in understanding of thermal grooving problem and provides an analytic solution which gives groove profile as a function of time and position using classical approach. After that time several improvements has been done by several researchers who follow the classical approach. In this review article we briefly discuss these concepts and conclude by giving examples of experimental observations compared with theoretical calculations.

It should be mentioned here that the classical approach indeed violates formation of non-equilibrium grooves and unable to describe transient states during grooving. A curious reader may refer to excellent papers by Suo [5], Ramasubramaniam and Shenoy [34], Ogurtani [35], Ogurtani and Oren [51] for a variational formulation of the problem and Ogurtani [52] for a complete irreversible thermo-kinetics treatment of solid surfaces and interfaces with triple junction singularities which is not intended to be included to this review.

REFERENCES

1. Mullins WW, Shewmon PG. The kinetics of grain boundary grooving in copper. Acta Metallurgica, 7, 3 (1959) 163–170. doi: 10.1016/0001–6160(59)90069–0.
2. Balluffi RW, Allen SM, Carter WC. Kinetics of Materials. John Wiley & Sons, Inc., Hoboken, NJ, USA, 2005. doi: 10.1002/0471749311.
3. Mullins WW. Theory of thermal grooving. Journal of Applied Physics, 28, 3 (1957) 333. doi: 10.1063/1.1722742.
4. Sun B, Suo Z, Yang W. A finite element method for simulating interface motion–I. Migration of phase and grain boundaries. Acta Materialia, 45, 5 (1997) 1907–1915. doi: 10.1016/S1359–6454(96)00323–0.
5. Suo Z. Motions of microscopic surfaces in materials. Advances in Applied Mechanics, 33 (1997) 193–294. doi: 10.1016/S0065–2156(08)70387–9.
6. Herring C. The physics of powder metallurgy. (Kinston WE) (p. 143). McGraw–Hill, New York, USA, 1951.
7. Gibbs W. The Collected Works of J. Willard Gibbs, Vol. I Thermodynamics. Yale University Press, New Haven, USA, 1948.
8. Defay R, Prigogine I. Surface tension and adsorption. (A. Bellemans). John Wiley & Sons., New York, USA, 1966.
9. Mullins WW. Solid surface morphologies governed by capillarity. In Metal Surfaces: Structure, Energetics and Kinetics (p. 17), ASM, Cleveland, OH, USA, 1963.
10. Robertson WM. Grain–boundary grooving by surface diffusion for finite surface slopes. Journal of Applied Physics, 42, 1 (1971) 463. doi: 10.1063/1.1659625.
11. Zhang W, Schneibel JH. Numerical simulation of grain–boundary grooving by surface diffusion. Computational Materials Science, 3, 3 (1995) 347–358. doi: 10.1016/0927–0256(94)00073–L.
12. Khenner M, Averbuch A, Israeli M, Nathan M, Glickman EE. Level set modeling of transient electromigration grooving. Computational Materials Science, 20,2 (2001) 235–250. doi: 10.1016/S0927–0256(00)00179–8.
13. Hackney SA, Ojard G. Grain boundary grooving at finite grain size. Scripta Metallurgica, 22,11 (1988) 1731–1735. doi: 10.1016/S0036–9748(88)80274–6.
14. Khenner M. Numerical simulation of grain–boundary grooving by level set method. Journal of Computational Physics, 170, 2 (2001) 764–784. doi: 10.1006/jcph.2001.6760.
15. Srolovitz DJ, Safran SA. Capillary instabilities in thin films. I. Energetics. Journal of Applied Physics, 60, 1 (1986) 247. doi: 10.1063/1.337689.
16. Huang P, Li Z, Sun J. Finite element analysis for surface

diffusion–controlled shape instabilities of plate–like grains. Computational Materials Science, 20,1 (2001) 66–76. doi: 10.1016/S0927–0256(00)00126–9.
17. Ogurtani TO, Akyildiz O. Grain boundary grooving and cathode voiding in bamboo–like metallic interconnects by surface drift diffusion under the capillary and electromigration forces. Journal of Applied Physics, 97, 9 (2005) 093520. doi: 10.1063/1.1883305.
18. Shenoy VB, Freund LB. A continuum description of the energetics and evolution of stepped surfaces in strained nanostructures. Journal of the Mechanics and Physics of Solids, 50, 9 (2002) 1817–1841. doi: 10.1016/S0022–5096(02)00015–7.
19. Jeong H, Williams, ED. Steps on surfaces: experiment and theory. Surface Science Reports, 34, 6–8 (1999) 171–294. doi: 10.1016/S0167–5729(98)00010–7.
20. Mykura H. The variation of the surface tension of nickel with crystallographic orientation. Acta Metallurgica, 9, 6 (1961) 570–576. doi: 10.1016/0001–6160(61)90160–2.
21. Bonzel HP, Mullins WW. Smoothing of perturbed vicinal surfaces. Surface Science, 350,1–3 (1996) 285–300. doi: 10.1016/0039–6028(95)01111–0.
22. Rabkin E, Klinger L, Semenov VN. Grain boundary grooving at the singular surfaces. Acta Materialia, 48, 7 (2000) 1533–1540. doi: 10.1016/S1359–6454(99)00432–2.
23. Klinger LM, Rabkin E. The effect of stress on grain boundary interdiffusion in a semi–infinite bicrystal. Acta Materialia, 55, 14 (2007) 4689–4698. doi: 10.1016/j.actamat.2007.04.039.
24. Rabkin E, Klinger L. The fascination of grain boundary grooves. Advanced Engineering Materials, 3, 5 (2001) 277–282. doi: 10.1002/1527–2648(200105)3:53.0.CO;2–G.
25. Zhang W, Sachenko PP, Schneibel JH. Kinetics of thermal grain boundary grooving for changing dihedral angles. Journal of Materials Research, 17, 6 (2002) 1495–1501. doi: 10.1557/JMR.2002.0222.
26. Akyildiz O, Oren EE, Ogurtani TO. Mesoscopic nonequilibrium thermodynamics treat–ment of the grain boundary thermal grooving induced by the anisotropic surface drift diffusion, J. Mater. Sci., 46, 18 (2011) 6054–6064.
27. Zhang W, Sachenko PP, Gladwell I. Thermal grain boundary grooving with anisotropic surface free energies. Acta Materialia, 52, 1 (2004) 107–116. doi: 10.1016/j.actamat.2003.08.033.
28. Xin T, Wong H. A δ–function model of facets. Surface Science, 487, 1–3 (2001) L529–L533. doi: 10.1016/S0039–6028(01)01158–X.
27. Xin T, Wong H. Grain–boundary grooving by surface diffusion with strong surface energy anisotropy. Acta Materialia, 51, 8 (2003) 2305–2317. doi: 10.1016/S1359–6454(03)00039–9.
30. Xin T, Wong H. A spike–function model of facets. Materials Science and Engineering A, 364, 1–2 (2004) 287–295. doi: 10.1016/j.msea.2003.08.042.
31. Min D, Wong H. Grain–boundary grooving by surface diffusion with asymmetric and strongly anisotropic surface energies. Journal of Applied Physics, 99, 2 (2006a) 023515. doi: 10.1063/1.2159082.
32. Du P, Wong H. A delta–function model for axially symmetric crystals. Scripta Materialia, 55,12 (2006) 1171–1174. doi: 10.1016/j.scriptamat.2006.07.042.
33. Ogurtani, T. O. Dirichlet extremum problem associated with the asymmetric grain–boundary thermal grooving under the Dirac δ–type anisotropic surface stiffness in bicrystal thin solid films. Journal of Applied Physics, 102, 6 (2007) 063517. doi: 10.1063/1.2781574.
34. Ramasubramaniam A, Shenoy VB. On the evolution of faceted grain–boundary grooves by surface diffusion. Acta Materialia, 53 (2005) 2943–2956. doi: 10.1016/j.actamat.2005.03.013.
35. Ogurtani TO. Variational formulation of irreversible thermodynamics of surfaces and interfaces with grain–boundary triple–junction singularities under the capillary and electromigration forces in anisotropic two–dimensional space. Physical Review B, 73, 23 (2006a) 1–17. doi: 10.1103/PhysRevB.73.235408.
36. Verschaffelt JE. The thermomechanics of the superficial layer. I. Generalities; pure substances. Bulletins de l'Academie Royale des Sciences, des Lettres et des Beaux Arts de Belgique, 22 (1936) 373.
37. Guggenheim EA. Thermodynamics (3 ed., p. 46). North–Holland, Amsterdam, Holland, 1959.
38. Ogurtani TO, Akyildiz O, Oren EE. Morphological evolution of tilted grain–boundary thermal grooving by surface diffusion in bicrystal thin solid films having strong anisotropic surface Gibbs free energies. Journal of Applied Physics, 104, 1 (2008) 013518. doi: 10.1063/1.2952520.
39. Ogurtani TO. Thermal grain–boundary grooving in bicrystal thin solid films having strong anisotropic surface Gibbs free energy represented by the modified cycloid–curtate function. Journal of Crystal Growth, 311, 6 (2009a) 1584–1593. doi: 10.1016/j.jcrysgro.2009.01.084.
40. Sharma SK, Spitz J. Thermal grooving in thin silver films. Journal of Materials Science, 16, 2 (1981) 535–536. doi: 10.1007/BF00738649.
41. Tsoga A, Nikolopoulos P. Groove angles and surface mass transport in polycrystalline alumina. Journal of the American Ceramic Society, 77, 4 (1994) 954–960. doi: 10.1111/j.1151–2916.1994.tb07252.x
42. Tritscher P, Broadbridge P. Grain boundary grooving by surface diffusion: an analytic nonlinear model for a symmetric groove. Proceedings of the Royal Society: Mathematical and Physical Sciences (1990–1995), 450, 1940 (1995) 569–587. doi: 10.1098/rspa.1995.0101.
43. Schöllhammer J, Chang L, Rabkin E, Baretzky B, Gust W, Mittemeijer E. Measurement of the profile and the dihedral angle of grain boundary grooves by atomic force microscopy. Zeitschrift für Metallkunde, 90 (1999) 687–690.
44. Shin W, Seo W, Koumoto K. Grain–boundary grooves and surface diffusion in polycrystalline alumina measured by atomic force microscope. Journal of the European Ceramic Society, 18, 6 (1998) 595–600. doi: 10.1016/S0955–2219(97)00207–0.
45. Lee KY, Case ED. A comparison of theoretical and experimental profiles for thermally–induced grain–boundary grooving. The European Physical Journal Applied Physics, 8, 3 (1999) 197–214. doi: 10.1051/epjap:1999247.
46. Rabkin E, Gabelev A, Klinger L, Semenov VN, Bozhko SI. Grain boundary grooving in molybdenum bicrystals. Journal of Materials Science, 41, 16 (2006) 5151–5160. doi: 10.1007/s10853–006–0438–4.
47. Sachenko PP, Schneibel JH, Zhang W. Effect of faceting on the thermal grain–boundary grooving of tungsten.

Philosophical Magazine A, 82, 4 (2002) 815–829. doi: 10.1080/01418610208243204.
48. Sachenko PP, Schneibel JH, Zhang W. Observations of secondary oscillations in thermal grain boundary grooves. Scripta Materialia, 50, 9 (2004) 1253–1257. doi: 10.1016/j.scriptamat.2004.01.030.
49. Sachenko PP, Schneibel JH, Swadener JG, Zhang W. Experimental and simulated grain boundary groove profiles in tungsten. Philosophical Magazine Letters, 80, 9 (2000)627–631. doi: 10.1080/09500830050134345.
50. Munoz NE, Gilliss SR, Carter CB. The monitoring of grain–boundary grooves in alumina. Philosophical Magazine Letters, 84, 1 (2003) 21–26. doi: 10.1080/09500830310001614487.
51. Ogurtani TO, Oren EE. Irreversible thermodynamics of triple junctions during the intergranular void motion under the electromigration forces. International Journal of Solids and Structures, 42, 13 (2005) 3918–3952. doi: 10.1016/j.ijsolstr.2004.11.013.
52. Ogurtani TO. Mesoscopic nonequilibrium thermodynamics of solid surfaces and interfaces with triple junction singularities under the capillary and electromigration forces in anisotropic three–dimensional space. The Journal of chemical physics, 124, 14 (2006b) 144706. doi: 10.1063/1.2185625.